Superconductivity and anomalous magnetic properties of the double-doping $La_{1.85-2x}Sr_{0.15+2x}Cu_{1-x}Ru_xO_4$ $(0 \leqslant x \leqslant 0.3)$ compounds

Jing Xie, Jiyu Fan, Shun Tan, and Yuheng Zhang*
Hefei High Magnetic Field Laboratory, University of Science and Technology of China, Hefei 230026, People's Republic of China
(Received 11 December 2005; revised manuscript received 27 February 2006; published 16 May 2006)

The effect of Ru^{4+} substitution for Cu^{2+} in the double-doped $La_{1.85-2x}Sr_{0.15+2x}Cu_{1-x}Ru_xO_4$ $(0 \leqslant x \leqslant 0.30)$ samples have been investigated by means of IR, Raman, the temperature dependence of resistivity, and magnetization under field cooling and zero field cooling. It is surprisingly found that the critical dopant level is higher than that by the single-doping method; even up to $x=0.3$, it is still pure phase because the valence unbalance has been compensated through the double-doping method. With Ru^{4+} doping, the evolution of IR and Raman spectra are correspondent with the anomalous magnetic properties. The superconductive transition survives until $x=0.03$, and there exists spin glass freezing in $0.04 \leqslant x \leqslant 0.06$ samples, the cluster glass state in $0.08 \leqslant x \leqslant 0.175$ samples, and the imperfect long range antiferromagnetic state in $0.20 \leqslant x \leqslant 0.30$ samples. The origin of the suppressing superconductivity is ascribed to the localization of hole carriers in the Cu-O planes caused by Ru^{4+} ions rather than their spins.

DOI: 10.1103/PhysRevB.73.174515 PACS number(s): 74.25.Fy, 74.25.Ha, 74.72.Dn

I. INTRODUCTION

Since the discovery of high-temperature superconductivity in doped La_2CuO_4 was reported by Bednorz and Müller,[1] there has been renewed interest in the normal state (NS) properties. The study of NS transport properties is considered to be able to provide important clues to the basic mechanism responsible for the superconductivity. Elemental doping with different 3*d* and *sp* metals is one of effective ways to probe the superconductivity and magnetic properties as well as studying the relation between spin correlation and transport properties.[2–4] According to previous studies, the superconductive transition temperature T_c mainly depends on the crystallographic structure, carrier concentration, as well as substitutional impurities. One knows that conventional superconductors are very sensitive to magnetic element doping, while the cuprate superconductors seem not so sensitive to magnetic element doping.[5] Lately, a new kind of unconventional superconductor Sr_2RuO_4 was found by Maeno *et al.*[6] Because the Sr_2RuO_4 not only is a superconductor but a magnetic one, it immediately became a focus of attention. However, a thorough understanding of the electronic properties of that metallic transition-metal oxide still remains elusive as well as that of $La_{2-y}Sr_yCuO_4$ superconductor.[7] We notice that the Ru^{4+} ion is a magnetic one, meanwhile, both La_2CuO_4 and Sr_2RuO_4 possess the same crystalline of K_2NiF_4-type structure. Naturally, if the two superconductors could be synthesized in the same tetragonal lattice, it would be very favorable for the clarification of their superconductivity. In the early stage, Xiong *et al.* have investigated the superconductivity with Ru^{4+} substitution for Cu^{2+} in $La_{1.85}Sr_{0.15}CuO_4$,[8] however, the valence unbalance induced by the high-valance Ru^{4+} ions makes it hard to obtain the high-dopant levels compounds, which poses an obstacle to best investigate the effect of Ru^{4+} doping. The critical dopant level they obtained is limited in $x=0.10$, therefore we design the double doping $La_{1.85-2x}Sr_{0.15+2x}Cu_{1-x}Ru_xO_4$ $(0 \leqslant x \leqslant 0.30)$ system to avoid inducing valance mismatch and gain the high-doping samples simultaneously, utilizing more Sr^{2+} doping to compensate the decrease of carrier concentration induced by Ru^{4+} doping. In this paper, we further investigate the magnetic properties of these compounds for a better understanding of the effect of Ru^{4+} doping. The experiments show that all the samples are pure phase until x up to 0.30 and the superconductivity survives until x up to 0.03. Furthermore, it is interesting that the spin glass freezing like behavior occurs in $0.04 \leqslant x \leqslant 0.06$ samples, the cluster glass state appears in $0.08 \leqslant x \leqslant 0.175$ samples, and the imperfect long range antiferromagnetic state exhibits in $0.20 \leqslant x \leqslant 0.30$ samples. We also verify that the suppression of superconductivity originates from the hole carriers localization in the Cu-O planes rather than the magnetic pair-breaking effect.

II. EXPERIMENTS

A series of samples with general formula $La_{1.85-2x}Sr_{0.15+2x}Cu_{1-x}Ru_xO_4$ $(0 \leqslant x \leqslant 0.3)$ were prepared by a conventional solid-state reaction method. Appropriate amounts of dried La_2O_3 (preheated at 800 °C for 12 h), $SrCO_3$, CuO, and RuO_2 were ground in an agate mortar. The mixtures were reacted in alumina crucible at 900 °C for 24 h with an intermediate grinding. Then they were reheated at 1000 °C for another 24 h. After ground, the mixture was pressed into pellets and sintered in air at 1100 °C for 24 h, then cooled down to room temperature with the furnace. Powder x-ray diffraction (XRD) (Rigaku-D/max-A) at room temperature was employed to check the structure and phase purity. Magnetic measurements were performed on a superconducting quantum interference device (SQUID). The Raman spectrum experiment was conducted by a SPEX-1403 spectrometer of back reflection geometric layout. The measurements of infrared transmission spectra were carried out with powder samples in the frequency range from 350 to 4000 cm^{-1}.

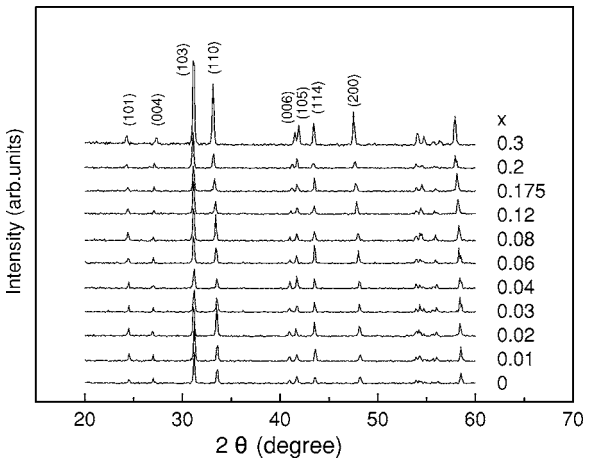

FIG. 1. XRD patterns of the $La_{1.85-2x}Sr_{0.15+2x}Cu_{1-x}Ru_xO_4$ ($0 \leqslant x \leqslant 0.30$) samples at room temperature.

III. RESULTS AND DISCUSSION

A. Structure

1. XRD patterns and lattice parameter

XRD (Fig. 1) analysis confirms that all the double-doping samples with x up to 0.30 are crystallized in single phase with a K_2NiF_4-type structure. They can be indexed with a tetragonal lattice structure. Table I presents the values of the lattice parameters "a," "c" and the ratio "c/a" versus x for the $La_{1.85-2x}Sr_{0.15+2x}Cu_{1-x}Ru_xO_4$ series. The lattice parameters were determined from the d values of XRD peaks by a standard least-squares refinement method. Obviously the lattice parameter "a" increases continuously while the parameters "c" and the ratio "c/a" monotonously decrease as x increases. These results verify the Cu^{2+} ions are substituted definitely by Ru^{4+} ions. The ratio of "c/a" is generally used to characterize the Jahn-Teller distortion of the oxygen octahedron around Cu^{2+} ions. The decreasing "c/a" indicates that the Ru doping leads to the release in the Jahn-Teller distortion of the CuO_6 octahedron, which is consistent with the previous reports.[9,10]

2. IR and Raman spectra

In order to further explore the effect of Ru^{4+} doping on the matrix structure, the vibration spectra in $Cu(Ru)O_6$ octahedrons have been investigated by means of IR and Raman, because the vibration modes are sensitive to the substitution. In IR spectra (Fig. 2), the strong absorption peak appearing around 505 cm^{-1} is assigned to A_{2u} stretching mode of apical oxygen atoms [O(2)] in the CuO_6 octahedrons.[11–15] With increasing x, the peak slightly shifts from 505 to 510 cm^{-1}.

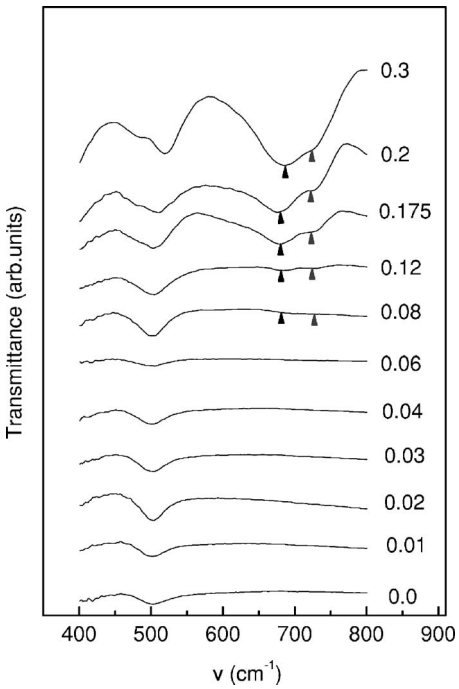

FIG. 2. Infrared phonon spectra of $La_{1.85-2x}Sr_{0.15+2x}Cu_{1-x}Ru_xO_4$ ($0 \leqslant x \leqslant 0.30$) samples at room temperature.

This is because the valence of the Ru ion is higher than that of the Cu ion, which causes the force constant of the Ru-O greater than that of Cu-O. Obviously the Cu-O(2) stretching modes are closely related to the Cu-O(2) bond distance and decreasing the bond distance of Cu-O(2) causes the phonon vibration mode shift to high frequencies, which is well understood based on the change of lattice parameter "c." When x reaches 0.08, a peak around 680 cm^{-1} appears and gradually enhances. It corresponds to the stretching mode of O(1) atoms in-plane on Cu-O-Ru.[12–15] The presence of this peak implies that the symmetry of the Cu-O plane in CuO_6 octahedrons near Ru^{4+} has been contorted in the horizontal planes. Thereby the peak at 680 cm^{-1} is excited. The enhancement of its intensity implies the amount of the contorted CuO_6 octahedrons increases. Around 730 cm^{-1}, a new peak appears when $x \geqslant 0.08$, which is obviously attributed to the stretching vibration mode of O(1) atoms in-plane on Ru-O-Ru.

In Raman spectrum (Fig. 3), only one strong Raman mode at 430 cm^{-1} can be clearly observed in the undoped sample. When $x \geqslant 0.01$, two weak peaks around 490 and 773 cm^{-1} appear and become more and more pronounced while the peak at 430 cm^{-1} gradually weakens and completely vanishes when $x=0.12$, meanwhile, another strong peak at 700 cm^{-1} appears when $x=0.08$ and gets more intensive

TABLE I. Cell parameters of the $La_{1.85-2x}Sr_{0.15+2x}Cu_{1-x}Ru_xO_4$ series.

Content (x)	0	0.01	0.03	0.04	0.08	0.12	0.175	0.2	0.3
a (Å)	3.77215	3.77153	3.77511	3.77594	3.78307	3.79305	3.80104	3.81191	3.83092
c (Å)	13.20043	13.20172	13.19446	13.18588	13.1868	13.14276	13.14396	13.14535	13.08026
c/a	3.49945	3.50036	3.49512	3.49208	3.48574	3.46496	3.45799	3.44849	3.41439

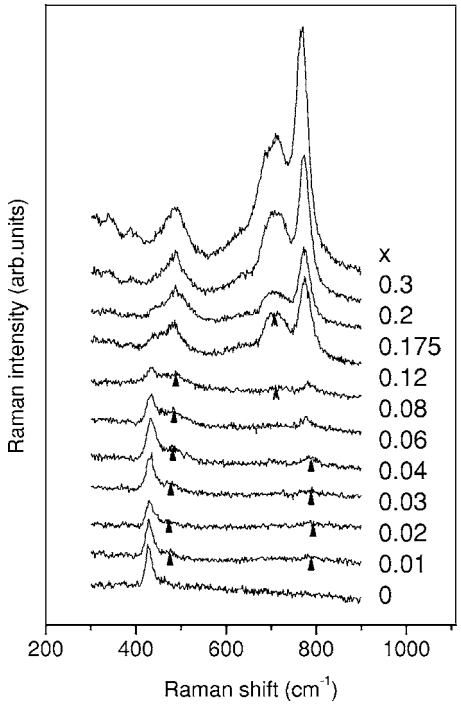

FIG. 3. Raman scattering spectra of $La_{1.85-2x}Sr_{0.15+2x}Cu_{1-x}Ru_xO_4$ $(0 \leqslant x \leqslant 0.30)$ samples at room temperature.

when $x \geqslant 0.12$. The 430 cm^{-1} peak is A_{1g} mode with the symmetric vibration of the apical oxygen atom O(2) along the c axis in CuO_6 octahedrons.[16] The 773 cm^{-1} peak is the vibration of Ru-O-Cu associated with the four O(1) atoms in plane, having A_1 symmetry in the orthorhombic system.[17] Because the force constant of Ru-O(2) is greater than that of Cu-O(2), it produces a relatively strong peak at 490 cm^{-1}. With more tetravalent Ru^{4+} ions introduced into the Cu-O planes, the intensity of the peak at 490 cm^{-1} enhances while that of the peak at 430 cm^{-1} weakens. Meanwhile the intensity of the peak at 773 cm^{-1} is enhanced gradually as x increases, obviously this peak is contributed by the vibration of Ru-O-Cu in plane. When $x \geqslant 0.08$, the appearance of a new 700 cm^{-1} peak would be ascribed to the vibration of the Ru-O-Ru in plane. This means there exists adjacent Ru^{4+} ions. Because both IR and Raman vibration modes are closely related to the Cu-based K_2NiF_4 structure; i.e., $(La/Sr)_2CuO_4$, the absence of each mode splitting into two modes of different frequencies upon increasing doping reveals that the Ru^{4+} dopant does not lead to the change in the structure and the Ru^{4+} ions can match the matrix closely. The results of Raman and IR spectra further verify that the Ru^{4+} ions are exactly introduced into the lattices with higher dopant levels $x=0.30$.

B. Magnetism

In view of the magnetism of Ru^{4+} ions, it will bring effect into the LSCO system. To study it, the temperature dependence of magnetization has been investigated at a temperature range from 4.2 to 200 K. In Fig. 4, the $M-T$ curves are displayed. The undoped sample exhibits a typical superconductive transition [Fig. 4(a)]. The magnetization nearly keeps unchanged and equals zero when the temperature decreases from 200 K to T_c ($T_c=37$ K), and then abruptly drops to negative value below T_c. For the low-doped samples, the onset temperature of superconductivity T_c^{onset} is 30 K for

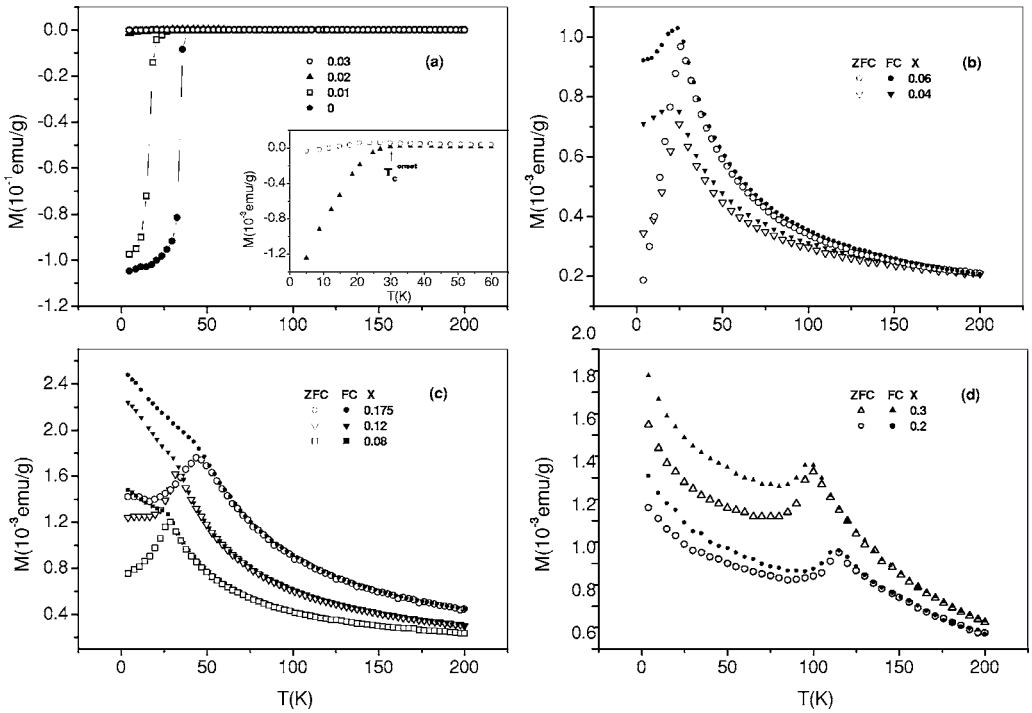

FIG. 4. Temperature dependence of (a) the zero-field-cooling magnetization ($H=100$ Oe) for the samples with $0 \leqslant x \leqslant 0.03$, and (b)–(d) M under ZFC and FC for the samples with $0.04 \leqslant x \leqslant 0.30$; the inset of (a) shows the amplified view for the samples with $x=0.02$ and 0.03.

both $x=0.01$ and 0.02. Their magnetic behaviors above T_c^{onset} are quite similar to that of undoped sample. Moreover the width of the superconductive transition $[\Delta T(\text{K})=T(90\%M)-T(10\%M)]$ is widened with increasing x. For $x=0.03$ sample, the value of magnetization is positive at room temperature and enhances with decreasing temperature. After reaching maxima at T_c^{onset} (24 K), M sharply drops to negative value. For $x\geqslant 0.04$ samples, M is positive within whole measured temperature range and increases with the decrease of temperature, then it abruptly drops at T_p at which it reaches maximum. Thus form a cusp on the $M-T$ curves [see Figs. 4(b)–4(d)]. The T_p is 24, 24, 26, 35.5, and 45 K for $x=0.04$, 0.06, 0.08, 0.12, and 0.175, respectively. For the samples with $x=0.20$ and 0.30, M keeps increasing after dropping at T_p. It is strange that T_p for $x=0.20$ and 0.30 is much higher than that for $x=0.175$, and $T_p=114$ for $x=0.20$ is higher than $T_p=101$ for $x=0.30$. Since no negative magnetization can be observed in the samples with $0.04\leqslant x\leqslant 0.30$, whether the drop of M is caused by the formation of cluster glass state as reported for cobaltites,[19] manganites,[20] and ruthenates.[18] To clarify these complex and interesting phenomena, we measured the field-cooling (FC) $M-T$ for the samples showing no negative magnetization to shed light on this question. In Fig. 4(b), the ZFC and FC curves for the samples with $x=0.04$ and 0.06 are given. The magnetization curves show indications of spin glass like freezing at the maxima in the ZFC and FC curves as several examples of spin glass systems that show a decreasing FC magnetization at temperatures below the freezing temperature.[21] In $0.08\leqslant x\leqslant 0.175$ samples, the ZFC and FC curves form typical "λ″ shape [in Fig. 4(c)], which is typically characteristic of the cluster glass state. These denote that the existence of ferromagnetism (FM) correlation in the $0.04\leqslant x\leqslant 0.175$ samples. In $x=0.2$ and 0.3 samples, the ZFC and FC curves exhibit quite a different scenario. Both ZFC and FC curves not only show drop at T_p but also the value of M still remarkably increases below T_p as the way above T_p [see Fig. 4(d)]. Moreover T_p gradually enhances from $x=0.04$ to 0.175, after that it dramatically increases from $x=0.175$ to 0.20, subsequently decreases for the $x=0.30$ sample. This implies the appearance of antiferromagnetism (AFM) for $x=0.20$ and 0.30 samples.

For further understanding the magnetic behaviors, we plot $1/M-T$ curves for $0.04\leqslant x\leqslant 0.30$ samples (see Fig. 5) The experimental data accord with linearity quite well. That follows the Curie law. Considering the difference between the transfer energy of Cu-O and Ru-O, the interaction between Cu and Ru ions is impossible. Therefore, it is more reasonable to ascribe the magnetism to the interaction between the magnetic Ru^{4+} ions. For the low-doped samples with $0.01\leqslant x\leqslant 0.06$, the Ru^{4+} ions are distributed individually and randomly in the matrix, which originates at the PM state. We analyze the magnetism of the sample with various Ru^{4+} concentration, according to Curie-Weiss law

$$\frac{M}{H}=\frac{c}{T-T_p} \tag{1}$$

where "c" is Curie constant, T_p is paramagnetic Curie temperature

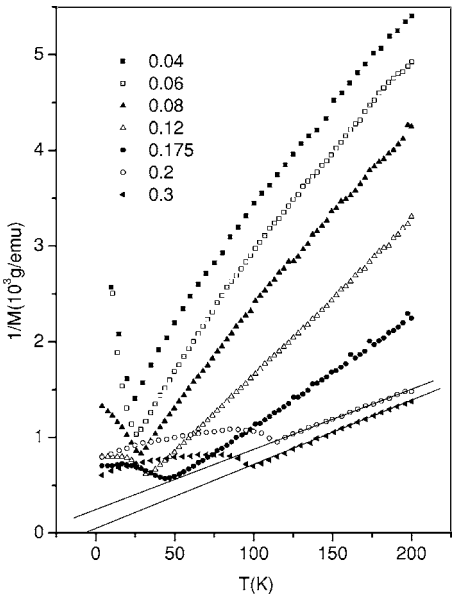

FIG. 5. $1/M$ versus T curves for $La_{1.85-2x}Sr_{0.15+2x}Cu_{1-x}Ru_xO_4$ $(0.04\leqslant x\leqslant 0.30)$ samples.

$$c=\frac{N\mu_{\text{eff}}^2}{3k}, \tag{2}$$

where N represents the number of Ru^{4+} ions in per gram sample. μ_{eff} is the effective magnetic moment of the Ru^{4+} ion. The curies constant "c" can be extracted from Fig. 5, then we can yield the $\mu_{\text{eff}}\approx 4.2\ m\mu_B$ for $x=0.04, 0.06$ through Eq. (2). It contributes to the (PM) state in the systems and the spin glass freezing.

For the samples with $0.08\leqslant x\leqslant 0.175$, the spins of all Ru^{4+} ions are in PM state at $T>T_p$, while FM clusters are formed when $T<T_p$. Evidently, this stems from the existence of adjacent Ru^{4+} ions and is in correspondence with above Raman analysis. Raman results show that there exist adjacent Ru^{4+} ions at $x\geqslant 0.08$, which corresponds precisely to the occurrence of FM correlation. However the number of the adjacent Ru^{4+} ions is too small to form an ordering state, and the FM coupling is fragile and unstable. When x up to 0.20, more Ru^{4+} ions get adjacent to each other, the coupling between Ru^{4+} ions is enhanced and they order in percolating but imperfect long range antiferromagnetic structures. Moreover, the extrapolated lines of the $1/M-T$ curves in Fig. 5 intersecting the negative x axis for the samples with $x=0.20$ and 0.30 also verifies the existence of the AFM state. Since there still exists nonadjacent Ru^{4+} ions, hence below T_p, their magnetism mainly contributed to the PM state. So the value of M still increases with decreasing temperature, which is clearly illustrated in Fig. 4(d). Here, it should be emphasized that FM clusters cannot be formed as that in $0.08\leqslant x\leqslant 0.175$ samples since the remaining Ru^{4+} ions are distributed individually and randomly in the matrix. The AFM correlation between Ru^{4+} ions is in accordance with that reported in the ruthenates with K_2NiF_4-type structure.[22] As for the decrease of T_p from $x=0.20$ to 0.30, that is because AFM order in the sample with $x=0.30$ is compara-

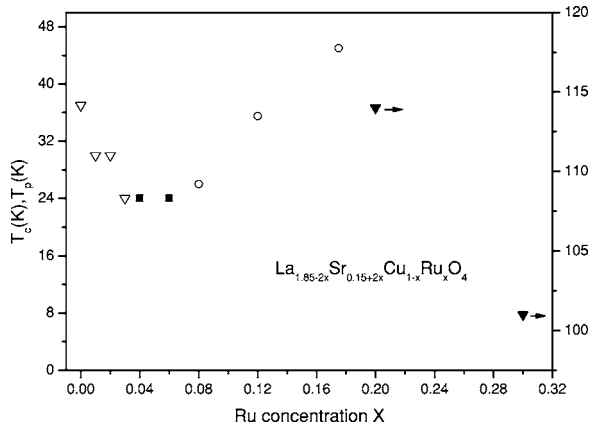

FIG. 6. T_c and T_p versus Ru concentration x for $La_{1.85-2x}Sr_{0.15+2x}Cu_{1-x}Ru_xO_4$ ($0 \leqslant x \leqslant 0.30$) samples; superconductive transition temperature T_c (∇), temperature shows spin glass freezing ($\blacksquare$), temperature appearing FM correlation ($\bigcirc$), temperature occurring AFM ordering ($\blacktriangledown$).

tively longer than that in the sample with $x=0.20$, as we know, the formation of the longer range ordering needs much lower temperature.[23,24]

From the above analysis, we suggest that the Ru^{4+} ions are randomly distributed in the matrix, and there exists spin-glass-like behavior for the samples with $0.04 \leqslant x \leqslant 0.06$. For the samples with $0.08 \leqslant x \leqslant 0.175$, due to the existence of adjacent Ru^{4+} ions, the FM correlation between them is formed in the PM background, so the cluster glass state is exhibited. For the sample with $x=0.2$ and 0.3, as more adjacent Ru^{4+} ions are introduced, the comparatively stable AFM coupling replaces the unstable FM correlation in the PM background. Figure 6 shows T_c (the temperature appearing superconductive transition) and T_p (the temperature occurring FM cluster or AFM ordering) dependence of Ru^{4+} concentration x.

C. Suppression of superconductivity

Xiao et al[25] and Bulut et al[26] have argued that the suppression of superconductivity by doping transition or *sp* elements on the Cu^{2+} site is consistent with the magnetic pair-breaking effect. As given by the conventional Abrikosov and Gor'kov theory,[27] this magnetic pair-breaking effect can be expressed in the form

$$\ln \frac{T_c}{T_{co}} = \Psi\left(\frac{1}{2}\right) - \Psi\left(\frac{1}{2} + \frac{2J^2S(S+1)N(E_F)x}{2k_BT_c}\right), \qquad (3)$$

where T_{co} is the value of T_c at dopant concentration $x=0$, J the exchange integral between the spin of the hole of oxygen atom and that of $3d$ elements, S the spin quantum number of the $3d$ element after substitution, $N(E_F)$ the density of states at the Fermi energy level, and Ψ the differential of the Γ function. When x is very small, the expression above gives a linear dependence of T_c on x as

$$T_{co} - T_c = \frac{\Pi^2 J^2 S(S+1)N(E_F)x}{2k_B} = Ax. \qquad (4)$$

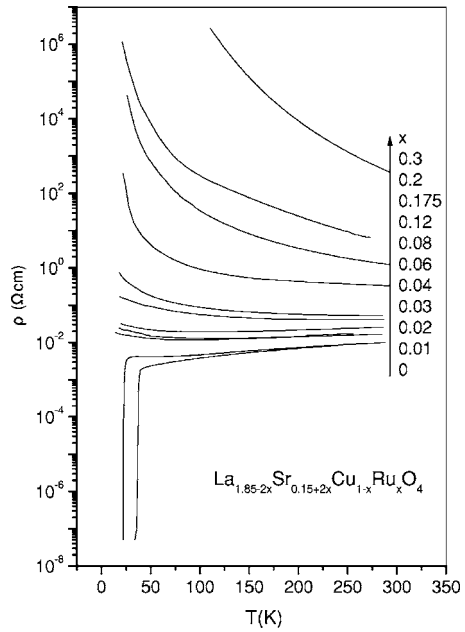

FIG. 7. Temperature dependence of resistivity for $La_{1.85-2x}Sr_{0.15+2x}Cu_{1-x}Ru_xO_4$ ($0 \leqslant x \leqslant 0.30$) samples.

Figure 6 shows a plot of T_c and T_p versus x for our results as compared to the prediction of the magnetic pair-breaking mechanism. Obviously, our experimental data deviate from linearity, and the results differ from the magnetic pair-breaking theoretical expectation. So the suppression of superconductivity in the $La_{1.85-2x}Sr_{0.15+2x}Cu_{1-x}Ru_xO_4$ system cannot be ascribed to the magnetic pair-breaking effect but the localization of carriers. When the impurity elements are introduced into the CuO_2 plane, the local number density of the electrons around the impurity atoms is enhanced. The interaction between the electrons of impurity atoms and the holes of the neighboring oxygen atoms will cause the holes to lose their itinerancy and prevent them from condensing into pairs, then the superconductivity is suppressed.

D. Resistivity

In Fig. 7, the curves of the temperature dependence of the resistivity for the $La_{1.85-2x}Sr_{0.15+2x}Cu_{1-x}Ru_xO_4$ system are given. It can be observed that the resistivity gradually enhances with the increasing Ru concentration. The samples with $x=0$ and 0.01 exhibit a typical superconductive transition in which the resistivity violently drops to zero. The samples with $x=0.03, 0.04$ exhibit a metallic behavior at the high temperature region and a semiconductorlike behavior at the low temperature region. For the sample with $x \geqslant 0.06$, they are all semiconductorlike at the whole temperature region. The typical superconductive transition can be only perceived for the samples with $x<0.02$, however, compared with the $M-T$ curves in which the superconductive transition survives until $x=0.03$. From Fig. 4(a) we can see that the value of M for $x=0.03$ sample at 4.2 K is one order of magnitude less than that of $x=0.02$ sample and three orders of magnitude less than those of $x=0$ and $x=0.01$ samples, which indicates that the superconductive segment in the

sample with $x=0.03$ is disjointed and too rare to be recorded by the measurement of resistivity.

IV. CONCLUSIONS

In summary, the structure and magnetic properties of the $La_{1.85-2x}Sr_{0.15+2x}Cu_{1-x}Ru_xO_4$ systems were studied in this paper. The higher critical doping levels up to $x=0.30$ for our double-doped systems are obtained due to the charge carrier compensation effect. At lower Ru^{4+} concentration with $x \leqslant 0.03$, the superconductive transition still survives. With increasing Ru^{4+} concentration, there exhibits the spin glass freezing in $0.04 \leqslant x \leqslant 0.06$, and the FM correlation between adjacent Ru^{4+} is formed in $0.08 \leqslant x \leqslant 0.175$ samples. Subsequently, the comparatively stable but imperfect long range AFM correlation substitutes the unstable FM correlation in the PM background due to more Ru^{4+} ions getting adjacent to each other. The magnetic properties of $La_{1.85-2x}Sr_{0.15+2x}Cu_{1-x}Ru_xO_4$ at low temperature is peculiar to that doped with other magnetic ions, such as $Mn^{4+}Co^{3+}$ ions.[28,29] Compared with the magnetic pair-breaking mechanism, the suppression of superconductivity is more reasonable to ascribe to the localization of hole carriers caused by Ru^{4+} ions rather than theirs spins.

ACKNOWLEDGMENTS

This work is supported by the National Natural Science Foundation of China through Grant No. 10334090, the Ministry of Science and Technology of China through Grant No. NKBRSF-619990646, and the National Center for Research and Development on Superconductivity.

*Electronic address: zhangyh@ustc.edu.cn

[1] J. G. Bednorz and K. A. Müller, Physica B & C **64B**, 189 (1986).
[2] N. Kakinuma, Y. Ono, and Y. Koike, Phys. Rev. B **59**, 1491 (1999).
[3] J. G. Naeini, X. K. Chen, J. C. Irwin, M. Okuya, T. Kimura, and K. Kishio, Phys. Rev. B **59**, 9642 (1999).
[4] Z. Mao, G. Xu, H. Yan, B. Wang, X. Qiu, and Y. Zhang, Phys. Rev. B **58**, 15116 (1998).
[5] N. Ishikawa, N. Kuroda, H. Ikeda, and R. Yoshizaki, Physica C **203**, 284 (1992).
[6] Y. Maeno, H. Hashimoto, K. Yoshida, S. Nishizaki, T. Fujita, J. G. Bednorz, and F. Lichtenberg, Nature (London) **37**, 532 (1994).
[7] J. J. Randall and R. Ward, J. Am. Chem. Soc. **81**, 2629 (1995).
[8] Y.M. Xiong, L. Li, X. G. Luo, H. T. Zhang, C. H. Wang, S. Y. Li, and X. H. Chen, J. Phys.: Condens. Matter **15**, 1693 (2003).
[9] J. M. Tarascon, L. H. Greene, P. Barboux, W. R. McKinnon, G. W. Hull, J. P. Orlando, K. A. Delin, S. Foner, and E. J. Mcniff, Phys. Rev. B **36**, 8393 (1987).
[10] H. Fujishita and M. Sato, Solid State Commun. **72**, 529 (1989).
[11] A. V. Bazhenov, T. N. Fursova, V. B. Timofeev, A. S. Cooper, J. P. Remeika, and Z. Fisk, Phys. Rev. B **40**, 4413 (1989).
[12] C. Zhang and Y. Zhang, Phys. Rev. B **67**, 153107 (2003).
[13] C. Zhang, C. Mu, and Y. Zhang, Phys. Lett. A **303**, 292 (2002).
[14] G. Xu, Q. Pu, Z. Zhang, and Z. Ding, J. Supercond. **14**, 509 (2001).
[15] G. Xu, Q. Pu, Z. Zhang, and Z. Ding, J. Supercond. **15**, 141 (2002).
[16] M. Mostoller, J. Zhang, A. M. Rao, and P. C. Eklund, Phys. Rev. B **41**, 6488 (1990).
[17] F. Y. C. Liu, P. J. Picone, D. R. Gabbe, and H. P. Jenssen, Phys. Rev. B **39**, 2293 (1989).
[18] P. Ravindran, R. Vidya, P. Vajeeston, A. Kjekshus, H. Fjellvåg, and B. C. Hauback, Solid State Commun. **124**, 293 (2002).
[19] D. N. H. Nam, K. Jonason, P. Nordblad, N. V. Khiem, and N. X. Phuc, Phys. Rev. B **59**, 4189 (1999).
[20] L. Ghivelder, I. A. Castillo, M. A. Gusmao, J. A. Alonso, and L. F. Cohen, Phys. Rev. B **60**, 12184 (1999).
[21] T. Motohashi, V. Caignaert, V. Pralong, M. Hervieu, A. Maignan, and B. Raveau, Phys. Rev. B **71**, 214424 (2005).
[22] G. Cao, S. McCall, M. Shepard, J. E. Crow, and R. P. Guertin, Phys. Rev. B **56**, R2916 (1997).
[23] Anthony Arulraj, P. N. Santhosh, R. Srinivasa Gopalan, Ayan Guha, A. K. Ray Chaudhuri, N. Kumar, and C. N. R. Rao, J. Phys.: Condens. Matter **10**, 8497 (1998).
[24] Anthony Arulraj, R. Gundakaram, Amlan Biswas, N. Gayathri, A. K. Ray Chaudhuri, and C. N. R. Rao, J. Phys.: Condens. Matter **10**, 4447–4456 (1998).
[25] G. Xiao, M. Z. Cieplak, J. Q. Xiao, and C. L. Chien, Phys. Rev. B **42**, 8752 (1990).
[26] N. Bulut, D. Hone, D. J. Scalapino, and E. Y. Loh, Phys. Rev. Lett. **62**, 2192 (1989).
[27] A. A. Abrikosov and L. P. Gor'kov, Sov. Phys. JETP **12**, 1243 (1961).
[28] C. Zhang and Y. Zhang, Phys. Rev. B **68**, 054512 (2003).
[29] Wu Huan, Ling Lin, Yudong Sun, Letian Ding, Weixian Wang, and Yuheng Zhang, Semicond. Sci. Technol. **18**, 277 (2005).